Published in final edited form as:
Nat Neurosci. 2009 October ; 12(10): 1285–1292. doi:10.1038/nn.2394.

Neuron-glia communication via EphA4/ephrinA3 modulates LTP through glial glutamate transport

Alessandro Filosa[1,*], **Sónia Paixão**[1,*,#], **Silke D. Honsek**[2], **Maria A. Carmona**[3], **Lore Becker**[4,5], **Berend Feddersen**[5], **Louise Gaitanos**[1], **York Rudhard**[6,$], **Ralf Schoepfer**[6], **Thomas Klopstock**[4,5], **Klas Kullander**[7], **Christine R. Rose**[2], **Elena B. Pasquale**[3], and **Rüdiger Klein**[1,#]

[1]Department of Molecular Neurobiology, Max-Planck Institute of Neurobiology, Am Klopferspitz 18, 82152 Martinsried, Germany

[2]Institute for Neurobiology, Heinrich-Heine-University Düsseldorf, Universitätsstrasse 1, 40225 Düsseldorf, Germany

[3]Burnham Institute for Medical Research, 10901 N. Torrey Pines Rd, La Jolla, CA 92037, USA

[4]German Mouse Clinic, Institute of Experimental Genetics, Helmholtz Zentrum München, German Research Center for Environmental Health (GmbH), Ingolstädter Landstrasse 1, D-85764 Munich, Germany

[5]Friedrich-Baur-Institute, Dept. of Neurology, University of Munich, Ziemssenstr. 1, D-80336 Munich, Germany

[6]Laboratory for Molecular Pharmacology, University College London, WC1E 6BT, London, UK

[7]Department of Neuroscience, Uppsala University, Box 587, 75123 Uppsala, Sweden

Abstract

Astrocytes are critical participants in synapse development and function, but their role in synaptic plasticity is unclear. Eph receptors and their ephrin ligands have been suggested to regulate neuron-glia interactions and EphA4-mediated ephrin reverse signaling is required for synaptic plasticity in the hippocampus. Here we show that long-term potentiation (LTP) at the CA3-CA1 synapse is modulated by EphA4 in the postsynaptic CA1 cell and by ephrinA3, a ligand of EphA4 that is found in astrocytes. Lack of EphA4 increases the levels of glial glutamate transporters and ephrinA3 modulates transporter currents in astrocytes. Pharmacological inhibition of glial glutamate transporters rescues the LTP defects in *EphA4* and *ephrinA3* mutant mice. Transgenic overexpression of ephrinA3 in astrocytes reduces glutamate transporter levels and produces focal dendritic swellings possibly caused by glutamate excitotoxicity. These results suggest that EphA4/ephrinA3 signaling is a critical mechanism for astrocytes to regulate synaptic function and plasticity.

[#]Corresponding authors: Rüdiger Klein (rklein@neuro.mpg.de). Sónia Paixão (paixao@neuro.mpg.de).
[$]Present address: Evotec AG, Schnackenburgallee 114, 22525, Hamburg, Germany
[*]equal contribution, in alphabetical order

AUTHOR CONTRIBUTIONS

A.F. designed, performed, analyzed most of the electrophysiology experiments and co-wrote the manuscript. S.P. designed, performed, analyzed the biochemical and quantitative anatomical studies and co-wrote the manuscript. S.D.H. and C.R.R. designed, performed and analyzed the astrocyte patch clamp recordings. M.A.C. and E.B.P. provided the ephrinA3$^{-/-}$ model, gave advice and aided in the interpretation of data. L.B., B.F. and T.K. performed and analyzed the induced seizure experiments. L.G. performed biochemical studies. Y.R. and R.S. provided the CA3-Cre mouse. K.K. provided *EphA4*$^{lx/+}$ ES cells. R.K. supervised the project, designed experiments and co-wrote the manuscript.

Interactions between neurons and astrocytes play critical roles in synapse/spine development and synaptic transmission [1]. Astrocytes release substances such as the matrix-associated protein thrombospondin to regulate synaptogenesis and a number of other factors, including the neurotransmitter D-serine, to regulate synaptic transmission [2, 3]. At excitatory synapses, astrocytes can sense synaptic activity by detecting glutamate released from presynaptic terminals and respond to this stimulus with the release of gliotransmitters that, in turn, modulate the activity of the neurons [2, 3]. Glutamate released into the synaptic cleft is cleared by a set of high-affinity transporters found on neurons and astrocytes. The glial transporters are responsible for clearing the majority of glutamate in the hippocampus [4]. Rapid removal from the extracellular milieu restrains spill-over of glutamate to nearby synapses and protects cells from glutamate excitotoxicity [4, 5]. Glutamate uptake by astrocytes is dynamic and increases during neuronal activity, including long-term potentiation [5–7]. However, the molecular mechanisms that regulate glutamate transport in astrocytes are poorly understood and, it is unclear to what extent astrocytes contribute to long term synaptic plasticity.

In mouse hippocampus and cerebral cortex, signaling by Eph receptor tyrosine kinases and their cell surface-associated ephrin ligands has been implicated in synapse and spine formation [8, 9]. B-type Eph receptors - which interact with transmembrane ephrinBs - regulate synapse/spine development, at least in part by trans-synaptic interaction with ephrinBs expressed in axon terminals [10]. In contrast, the A-type Eph receptor, EphA4, which has the potential to interact with both A-type and B-type ephrins, was suggested to interact with ephrinA3 expressed on astrocytic processes. Activation of EphA4 forward signaling reduces spine length, whereas inhibition of EphA4 signaling [11] increases spine length. Hence, astrocytes use the Eph/ephrin system to shape spine morphology and possibly synaptic function.

Eph/ephrin signaling also promotes certain forms of hippocampal synaptic plasticity independently of morphological changes [9]. At the CA3-CA1 synapse, both EphB2 and EphA4 are required for LTP; however, unlike the mechanism which promotes spine remodeling, both Eph receptors act in a kinase-independent fashion [12–14]. EphB2 may either act postsynaptically by interacting *in cis* with NMDA receptors [15] or in the axon terminal, where it trans-synaptically interacts with postsynaptic ephrinBs [9, 16]. Unlike EphB2, EphA4 does not appear to interact with NMDA receptors [15] and the mechanism by which it promotes LTP is unknown.

Here we show that only post-synaptic/dendritic, but not axonal, EphA4 is required for certain forms of LTP. Loss of ephrinA3 affects the same forms of LTP and raises glutamate transporter currents in astrocytes. Loss of neuronal EphA4 increases, whereas transgenic overexpression of ephrinA3 in astrocytes decreases glial glutamate transporter levels. The LTP deficiency observed in both *EphA4* and *ephrinA3* mutants is rescued by blocking glial glutamate transporters. These results suggest that interactions between dendritic EphA4 and ephrinA3 control glial glutamate transport, which regulate synaptic glutamate concentration and postsynaptic depolarization and ultimately modulate the expression of LTP at excitatory synapses.

RESULTS

EphA4 is required for LTP in post-synaptic CA1 cells

To remove EphA4 from sub-regions of the hippocampus, we used a conditional allele of EphA4 (*EphA4*^{lx}; K.K., unpublished results). *PGK-Cre;EphA4*$^{lx/lx}$ mice, in which EphA4 is ubiquitously deleted, displayed phenotypes previously described in *EphA4* null mutants (Suppl. Fig. S1) [17]. Although EphA4 expression in control *EphA4*$^{lx/lx}$ mice is reduced to 15–20% compared to +/+ mice (Suppl. Fig. S1a), this reduction does not cause phenotypic

alterations (Suppl. Fig. S1). We also did not find alterations in CA3-CA1 LTP in control *EphA4*$^{lx/-}$ mice, which only had one intact EphA4 allele, compared to *EphA4*$^{lx/+}$ mice (Suppl. Fig. S1j,k). To generate CA1 pyramidal cell-specific *EphA4* knockout mice, we used the *R4Ag11CamKII-Cre* mouse line (CA1-Cre) [18] which displays full activity in CA1 at postnatal day (P) 31 (Fig. 1a–c). To generate CA3 pyramidal cell-specific EphA4 knockout mice, we used a new *KA1-Cre* knock-in mouse line, which expresses Cre from the endogenous *KA1* locus (CA3-Cre; Suppl. Fig. S2). The *CA3-Cre* line recombines in nearly all cells of CA3 and in a smaller fraction of dentate gyrus cells, starting from the first postnatal week (Fig. 1d–f). The recombination efficiencies in the CA1-Cre and CA3-Cre lines, quantified by *in situ* hybridizations (Fig. 1g–i), were approximately 80% for both lines (CA1/CA3 ratio in *CA1-Cre; EphA4*$^{lx/-}$=20% ± 12%, compared to *EphA4*$^{lx/-}$=91% ± 4%; CA3/CA1 ratio in *CA3-Cre;EphA4*$^{lx/-}$=24% ± 4%, compared to *EphA4*$^{lx/-}$=116% ± 7%; n=3–5 mice; *t*-test, p<0.0001).

CA1-Cre;EphA4$^{lx/-}$ and *CA3-Cre;EphA4*$^{lx/-}$ mice exhibited no gross developmental abnormalities. Before analyzing synaptic plasticity, we analyzed potential morphological alterations and basic synaptic parameters. Biolistic labeling with DiI in hippocampal slices did not reveal alterations in the morphology of dendritic spines in *CA1-Cre;EphA4*$^{lx/-}$ mice, compared to the *EphA4*$^{lx/-}$ controls, possibly due to the incomplete recombination efficiencies (data not shown). Extracellular recordings in acute hippocampal slices of the CA3-CA1 pathway in both conditional mutants did not reveal significant deficiencies in the slopes of field excitatory postsynaptic potentials (fEPSPs) nor in paired-pulse facilitation (PPF) at various interstimulus intervals (ISIs) (Suppl. Fig. S3). AMPA and NMDA receptor functions, as well as CaMKIIα protein levels, were tested in *EphA4* null mice and found to be unaffected (Suppl. Fig. S4k,l). To investigate a requirement for either postsynaptic (CA1) or presynaptic (CA3) EphA4 in LTP, we used theta-burst stimulation (TBS). After recording a stable baseline, three TBS were given to fibers of the CA3 presynaptic neurons and LTP was recorded from CA1 neurons for up to 60 min post stimulation. Comparison of *CA1-Cre;EphA4*$^{lx/-}$ mice with littermate *EphA4*$^{lx/-}$ controls revealed a marked reduction in LTP (Fig. 1j) comparable to the situation when EphA4 was removed postnatally from all pyramidal neurons of the forebrain (*CamKII-Cre;EphA4*$^{lx/-}$ mice; Suppl. Fig. S3g,h). In contrast, TBS-induced LTP was not altered in *CA3-Cre;EphA4*$^{lx/-}$ mice (Fig. 1k). These results demonstrate that EphA4 functions postsynaptically to regulate LTP at the CA3-CA1 synapse.

EphrinA3 is required for TBS-induced LTP

Dendritic EphA4 has been shown to respond to ephrinA3 expressed in astrocytes [11, 19] and, immunoelectron microscopic studies suggested that EphA4 is expressed mainly perisynaptically [20]. We therefore asked if ephrinA3 function is critical for LTP. We used an *ephrinA3* null mutant mouse which has alterations in spine morphology [19], but does not display significant defects in basal synaptic transmission parameters such as PPF, input-output ratios, amplitude and frequency of mEPSCs, suggesting that the observed spine alterations are not critical for basic synaptic functions (Fig. 2a,b; Suppl. Fig. S4). As for *EphA4* mutants, LTP induced by a TBS protocol was strongly reduced in *ephrinA3*$^{-/-}$ slices (Fig. 2c).

Interestingly, this LTP defect in *ephrinA3*$^{-/-}$ slices was specific for TBS and was not observed after tetanic stimulation (Fig. 2d). Therefore, the requirement of ephrinA3 for LTP is dependent on a stimulus protocol which is physiologically closer to what happens in the hippocampus during learning and memory [21] and suggests a direct, possibly signaling function of ephrinA3 in LTP. The requirement for TBS, but not tetanus-induced LTP, was

also observed in EphA4 mutant mice (Fig. 2e,f; Suppl. Fig. S3h). These findings suggest that EphA4 interacts with ephrinA3 to regulate TBS-induced LTP at the CA3-CA1 synapse.

Glial glutamate transporter regulation by EphA4/ephrinA3

Next, we reasoned that the EphA4 ectodomain may activate ephrinA3 reverse signaling in astrocytes, thereby modulating astrocytic functions that impact on LTP. Since glial glutamate transporters are known to regulate synaptic transmission by clearing glutamate from the synaptic cleft [5, 22], we investigated the expression of the glial glutamate/aspartate transporter (GLAST or EAAT1) and glutamate transporter subtype-1 (GLT1/EAAT2) in our mutant mice. A marked upregulation of GLAST protein levels and a modest increase in GLT-1 levels were observed in *EphA4*$^{-/-}$ brains compared to littermate controls (Fig. 3a–c). Levels of glial fibrillary acidic protein (GFAP) and the neuronal excitatory amino acid carrier-1 (EAAC-1/EAAT3) were not altered (Fig. 3a–c). Importantly, the upregulation of GLAST and GLT-1 was rescued in *EphA4*$^{EGFP/EGFP}$ mice, in which the cytoplasmic domain is replaced by GFP [12], suggesting that the EphA4 ectodomain was sufficient to maintain normal GLAST and GLT-1 levels (Fig. 3d–f). GLAST upregulation was also seen in dissected CA1 regions, but not CA3, of *CA1-Cre;EphA4*$^{lx/-}$ mice compared to littermate controls (Fig. 3g–i). Similar changes in GLAST and GLT-1 were observed in *ephrinA3*$^{-/-}$ mice [19]. These results suggest that the EphA4 ectodomain, presumably by interacting with ephrinA3, restricts the expression of glial glutamate transporters. These changes were not secondarily caused by an increase in astrocyte numbers in *EphA4*$^{-/-}$ mice and the regulation appeared to happen at the post-transcriptional level, since the levels of GLAST and GLT-1 mRNAs in *EphA4*$^{-/-}$ and *ephrinA3*$^{-/-}$ mice were similar to control mice (Suppl. Fig. S5).

The upregulation of glial glutamate transporter levels may result in increased glutamate transporter currents in mutant astrocytes. We performed whole-cell patch-clamp recordings from astrocytes in the *stratum radiatum* of *ephrinA3*$^{-/-}$ hippocampal slices. Transporter currents were evoked by endogenous release of glutamate from presynaptic terminals following Schaffer collateral stimulation. The mean peak amplitude of transporter currents normalized to the respective fiber volley in response to single pulse stimulation was significantly higher in *ephrinA3*$^{-/-}$ compared to littermate controls (Fig. 4a,c; Suppl. Fig. S6). Similar results were obtained with a TBS protocol (Fig. 4b,c; Suppl. Fig. S6), which had produced a much reduced LTP in *ephrinA3*$^{-/-}$ mice (Fig. 2). These results indicate that glutamate uptake by astrocytes in response to a single burst or a TBS protocol was significantly increased in *ephrinA3*$^{-/-}$ animals.

Glutamate concentration near synapses and effect on LTP

We next asked if elevated levels of glutamate transporters in astrocytes would decrease synaptic glutamate levels. To estimate synaptic glutamate concentrations, we performed whole-cell patch-clamp recordings from CA1 hippocampal neurons in acute slices in the presence of the low-affinity competitive AMPA receptor antagonist γ-D-glutamylglycine (γ-DGG). γ-DGG binds non-NMDA receptors with low affinity and with rapid dissociation kinetics comparable to the association kinetics of synaptically released glutamate [23, 24]. Thus, the degree of inhibition by γ-DGG is sensitive to the concentration of glutamate. If less glutamate is present, the inhibition by γ-DGG is stronger. We found comparable amplitudes and frequencies of miniature excitatory post-synaptic currents (mEPSCs) in slices derived from *EphA4*$^{-/-}$ mice and +/+ littermate controls (Fig. 5a; Suppl. Fig. S4a–d). γ-DGG reduced the amplitude of mEPSCs in *EphA4*$^{-/-}$ slices more than in +/+ controls (Fig. 5b), indicating that the levels of glutamate near synapses in *EphA4*$^{-/-}$ slices are reduced. These results suggest that the clearance of glutamate is more efficient in the EphA4 mutants, possibly due to the upregulation of glial glutamate transporters.

To test if the changes in glutamate concentration result in insufficient postsynaptic depolarization, we analyzed fEPSPs during high frequency stimulation. fEPSP slopes at the end of the first train of each TBS were significantly reduced in *CA1-Cre;EphA4*$^{lx/-}$ and *ephrinA3*$^{-/-}$, but not *CA3-Cre;EphA4*$^{lx/-}$ mice, compared to their respective controls (Fig. 5c–e). Next, we investigated the effects of blocking glutamate reuptake on LTP. We used (2S, 3S)-3-{3-[4-(trifluoromethyl)benzoylamino)benzyloxy}aspartate (TFB-TBOA) a non-transportable inhibitor that primarily inhibits GLT-1 and GLAST but also substantially targets the neuronal transporter EAAC1 [25]. If the LTP impairments were due to glutamate transporter upregulation, TFB-TBOA should rescue the LTP defects. Indeed, the application of TBS in the presence of TFB-TBOA induced similar amounts of synaptic potentiation in *CA1-Cre;EphA4*$^{lx/-}$ and *ephrinA3*$^{-/-}$ mice compared to their respective controls (Fig. 5f,g). Interestingly, the presence of TFB-TBOA also allowed normal post-synaptic depolarization in *CA1-Cre;EphA4*$^{lx/-}$ and *ephrinA3*$^{-/-}$ slices during the application of TBS (slope4/slope1: 1.23 ± 0.16 in *CA1-Cre; EphA4*$^{lx/-}$, n=9 slices, 7 mice versus 1.30 ± 0.08 in *EphA4*$^{lx/-}$, n=13 slices, 7 mice, *t*-test, p=0.7; 1.24 ± 0.19 in *ephrinA3*$^{-/-}$, n=12 slices, 8 mice versus 1.34 ± 0.12 in +/+, n=11 slices, 8 mice, *t*-test, p=0.7). These results suggest that the impaired LTP observed in *CA1-Cre;EphA4*$^{lx/-}$ and *ephrinA3*$^{-/-}$ mice is largely due to the reduced levels of glutamate near synapses, caused by increased glutamate transport into astrocytes.

Overexpression of ephrinA3 in astrocytes

To obtain further support for ephrinA3 regulating glial glutamate transport, we generated transgenic lines overexpressing ephrinA3 (fused to an HA epitope tag) in glial cells using the GFAP promoter [26] (Suppl. Fig. S7a). Two lines (Tg181, and Tg7047) produced viable offspring and were further analyzed. Based on qRT-PCR analysis, Tg181 hippocampi contained 4.5-times the normal ephrinA3 levels (Suppl. Fig. S7e). Anti-HA immunostaining of P30-60 brain sections revealed the typical scattered distribution expected for glial cells (Fig. 6a,b; Suppl. Fig. S7b,c). Endogenous EphA4 phosphorylation levels were higher in hippocampal lysates from Tg181 compared to littermate controls (Fig. 6c) indicating that the transgenic protein was functional and that EphA4 efficiently interacts with glial ephrinA3. We confirmed ephrinA3 overexpression in the fine processes of astrocytes by using a GFAP-GFP indicator line [26] (Fig. 6d–g).

To investigate the effects of transgenic ephrinA3 on endogenous glial glutamate transporters levels, we co-stained hippocampal sections from Tg181 with HA and GLAST or GLT1 antibodies (Fig. 6h–j, l–n). Areas of high, medium and low HA immunoreactivities were selected and average pixel intensities were compared to endogenous glial transporters levels. An inverse correlation was seen between HA and GLAST/GLT1 expression levels (Fig. 6k,o); similar reductions of glial glutamate transporter levels were observed in line Tg7047 which expressed lower levels of transgenic ephrinA3 than Tg181 (Suppl. Fig. S7), suggesting that modest overexpression of ephrinA3 above endogenous levels is sufficient to reduce glial glutamate transporter expression. To verify that the transgenic protein was not targeted to a subpopulation of astrocytes that express less glutamate transporters, we co-stained hippocampal sections from the GFAP-GFP indicator line with GFP and GLAST or GLT1 antibodies. We found that the expression of glutamate transporters did not correlate with the expression of GFP in astrocytes (Fig. 6p–s; Suppl. Fig. S7). These results indicate that ephrinA3 in astrocytes is sufficient to suppress glial glutamate transporter expression.

Reduction of glial glutamate transporters has previously been shown to increase synaptic glutamate concentrations and to cause epilepsy and neurodegeneration [27–29]. Excessive glutamate concentrations cause excitotoxicity which is reflected in dendritic beading and spine loss [30]. To assess the degree of dendritic beading in ephrinA3 transgenic mice, we performed biolistic labeling of neurons with DiI or intercrossed Tg181 with a transgenic line

(GFP-M) which expresses GFP in small neuronal subsets [31]. CA1 neurons in P29-31 hippocampal slices derived from Tg181 mice, but not from +/+ littermates, showed dendritic beading (Fig. 7a–d) with variable penetrance possibly due to variable expression of the transgene (38.84 ± 2.96% of swelling coverage, n=16 dendrites, 6 mice, in Tg181 versus 21.70 ± 5.71%, n=10 dendrites, 6 mice, in littermate +/+ controls, *t*-test, p=0.003). Neurons from line Tg181 also displayed significant spine loss (1.37 ± 0.06 spines/μm in Tg181, n=16 dendrites, 6 mice, versus 1.58 ± 0.07 spines/μm in control animals, n=10 dendrites, 6 mice, *t*-test, p=0.02), probably as an indirect consequence of beading [32]. Dendritic beading can also be induced in hippocampal slice cultures by application of agonists of ionotropic glutamate receptors [30]. In cultured slices derived from line Tg181 neurons did not contain dendritic beads. However, they were more sensitive to glutamate bath application than control slices (Fig. 7e–g). Deficiency in glial glutamate transporters results in increased sensitivity to pentylenetetrazole (PTZ)-induced seizures [28, 29]. Consistent with these reports, Tg181 mice displayed increased seizure severity and more whole-body myocloni after application of PTZ compared to controls (Fig. 7h,i). These results suggest that overexpression of ephrinA3 in astrocytes downregulated glutamate transporter levels, which caused glutamate excitotoxicity and exacerbated PTZ-induced seizures.

DISCUSSION

The results presented here show a novel mechanism by which astrocytes modulate neuronal plasticity in the CA1 region of the hippocampus. Astrocytes receive a signal from dendritic EphA4 receptors via ephrinA3, which prevents them from upregulating glial glutamate transporter expression to unphysiologically high levels. Dendritic EphA4 and ephrinA3 in astrocytes thereby control glutamate concentrations near synapses and promote LTP. In the absence of either dendritic/postsynaptic EphA4 or ephrinA3, glutamate transporter levels are increased (see also [19]) and glutamate is more efficiently removed during high frequency stimulation. As a consequence, peri- and extrasynaptic glutamate receptors [33, 34] might not be sufficiently activated, resulting in insufficient depolarization of the postsynapse and partial impairment of LTP. These findings are consistent with previous observations in the cerebellum where synaptic plasticity is controlled by the neuronal glutamate transporter EAAT4 [35, 36]. They also concur with previous observations that glutamate transporter levels are regulated by neuronal activity [7]. Induction of LTP in area CA1 was shown to increase both neuronal [37] and glial [6] glutamate uptake. It is therefore possible that neuronal activity regulates EphA4/ephrinA3 signaling to control glial glutamate transport and in this way fine tune synaptic transmission.

We cannot exclude the possibility that the observed changes in LTP are exacerbated by morphological changes. Previous studies in the hypothalamus have shown that reduced astrocyte coverage enhanced extracellular glutamate concentrations and activation of metabotropic glutamate receptors [24]. It is also possible that loss of EphA4/ephrinA3 changes the motility of astrocytic processes as previously suggested based on stimulations with Fc fusion proteins [38, 39]. However, we found that pharmacological inhibition of glutamate re-uptake rescued the LTP defects, arguing that the observed LTP defects in EphA4/ephrinA3 mutant mice were caused by deficiencies in acute signaling rather than by morphological alterations. The fact that LTP defects were only observed after TBS, but not tetanus, could be explained by the intrinsic capacity of transporters to clear glutamate. TBS consists of short trains of high frequency stimulations with interburst intervals of 200 ms, which lead to modest glutamate release and to glutamate concentrations that are sensitive to transporter levels [40]. We showed that transporter currents are higher in *ephrinA3*$^{-/-}$ than in control mice also under TBS conditions, suggesting that these modest glutamate elevations are cleared more efficiently than normal and thereby reduce the degree of postsynaptic depolarization during LTP induction. Using a stronger protocol, such as tetanus, which leads

to much higher glutamate release, may overwhelm the capacity of the transporters. In that case, the increase in glutamate transporters in mutant mice may be as ineffective as in control mice in buffering extracellular glutamate. Alternatively, tetanus stimulation may influence transporter currents by mechanisms independently of Eph/ephrin signaling.

EphA4 is expressed both pre- and postsynaptically [20], but here we discovered that only the postsynaptic fraction of EphA4 plays a role in LTP. Therefore, the previously suggested model of axonal EphA4 activating ephrinB reverse signaling in spines is probably incorrect [12]. To be able to activate ephrinBs, EphA4 would have to interact with ephrinBs *in cis* which we consider unlikely. Instead, the results in this study (see also [19]) suggest that EphA4 interacts with astrocytic ephrinA3. The requirement for postsynaptic, but not presynaptic, EphA4 could be explained by the fact that glial coverage at hippocampal synapses is asymmetrically distributed, with 3-fold more glial contact with spines compared to pre-synaptic boutons [41]. The role of EphA4 in LTP is independent of forward signaling [12] and therefore distinct from its role in spine morphogenesis [11]. It is likely that the EphA4 ectodomain activates ephrinA3 reverse signaling in astrocytes; however, the mechanism that regulates glial glutamate transporter levels downstream ephrinA3 is currently unknown. Since ephrinA3 mRNA is also detectable in pyramidal neurons (data not shown), we cannot formally rule out a function of ephrinA3 in hippocampal neurons.

What are the physiological and pathophysiological implications of our observations? Hippocampal LTP is a critical component of the cellular mechanisms underlying certain aspects of learning and memory [42]. *ephrinA3*$^{-/-}$ mice were shown to have impairments in certain behavioral tests requiring the hippocampus [19], suggesting that the regulation of glial glutamate transport and synaptic plasticity may be critical for certain forms of hippocampal learning. Moreover, the phenotypes described in the ephrinA3 transgenic lines suggest that mechanisms promoting ephrinA3 reverse signaling may contribute to lowering glutamate transporter expression, which results in glutamate excitotoxicity [27–29]. Dysfunction of glial glutamate transporters is implicated in the pathology of various neurological and neurodegenerative diseases such as epilepsy and amyotrophic lateral sclerosis (ALS) [3, 22]. Interestingly, the human VAPB protein, a diffusible ligand for Eph receptors and potential antagonist for ephrins, is associated with familial ALS [43]. It is tantalizing to speculate that mutations of VAPB enhance EphA4/ephrinA3 signaling, thereby causing the down regulation of glial glutamate transporters observed in ALS.

Supplementary Material

Refer to Web version on PubMed Central for supplementary material.

Acknowledgments

We thank M. Bösl and the transgenic core facility for the generation of transgenic mice; E. Kandel and F. Kirchhoff for transgenic mice; M. Klein, and O. Gökce for technical help; K. Deininger, C. Erlacher, V. Staiger, V. Stein and M. Traut for scientific input and suggestions; M. Korte, I. Kadow, V. Stein, J. Egea, and R. Fonseca for critical comments on the manuscript. S.P. was supported by a postdoctoral fellowship from FCT, Portugal, cofinanced by POCI 2010 and FSE. M.A.C. was supported by a fellowship from Fundación Española para la Ciencia y la Tecnología. This work was in part supported by grants from the EU (Endotrack), the Deutsche Forschungsgemeinschaft (SPP1172) and the Max-Planck Society (all to R.K.), the Wellcome Trust and the Biotechnology and Biological Sciences Research Council, UK (R.S.), the German National Genome Research Network (NGF N grant 01GR0430) (T.K.), and NIH grant HD025938 (E.B.P.).

References

1. Allen NJ, Barres BA. Signaling between glia and neurons: focus on synaptic plasticity. Current opinion in neurobiology. 2005; 15:542–548. [PubMed: 16144764]

2. Barres BA. The mystery and magic of glia: a perspective on their roles in health and disease. Neuron. 2008; 60:430–440. [PubMed: 18995817]
3. Halassa MM, Fellin T, Haydon PG. The tripartite synapse: roles for gliotransmission in health and disease. Trends in molecular medicine. 2007; 13:54–63. [PubMed: 17207662]
4. Bergles DE, Jahr CE. Glial contribution to glutamate uptake at Schaffer collateral-commissural synapses in the hippocampus. J Neurosci. 1998; 18:7709–7716. [PubMed: 9742141]
5. Tzingounis AV, Wadiche JI. Glutamate transporters: confining runaway excitation by shaping synaptic transmission. Nature reviews. 2007; 8:935–947.
6. Pita-Almenar JD, Collado MS, Colbert CM, Eskin A. Different mechanisms exist for the plasticity of glutamate reuptake during early long-term potentiation (LTP) and late LTP. J Neurosci. 2006; 26:10461–10471. [PubMed: 17035530]
7. Genoud C, et al. Plasticity of astrocytic coverage and glutamate transporter expression in adult mouse cortex. PLoS biology. 2006; 4:e343. [PubMed: 17048987]
8. Essmann CL, et al. Serine phosphorylation of ephrinB2 regulates trafficking of synaptic AMPA receptors. Nature neuroscience. 2008
9. Klein R. Bidirectional modulation of synaptic functions by Eph/ephrin signaling. Nature neuroscience. 2009; 12:15–20.
10. Kayser MS, Nolt MJ, Dalva MB. EphB receptors couple dendritic filopodia motility to synapse formation. Neuron. 2008; 59:56–69. [PubMed: 18614029]
11. Murai KK, Nguyen LN, Irie F, Yamaguchi Y, Pasquale EB. Control of hippocampal dendritic spine morphology through ephrin-A3/EphA4 signaling. Nature neuroscience. 2003; 6:153–160.
12. Grunwald IC, et al. Hippocampal plasticity requires postsynaptic ephrinBs. Nature neuroscience. 2004; 7:33–40.
13. Grunwald IC, et al. Kinase-independent requirement of EphB2 receptors in hippocampal synaptic plasticity. Neuron. 2001; 32:1027–1040. [PubMed: 11754835]
14. Henderson JT, et al. The receptor tyrosine kinase EphB2 regulates NMDA-dependent synaptic function. Neuron. 2001; 32:1041–1056. [PubMed: 11754836]
15. Dalva MB, et al. EphB receptors interact with NMDA receptors and regulate excitatory synapse formation. Cell. 2000; 103:945–956. [PubMed: 11136979]
16. Bouzioukh F, et al. Tyrosine phosphorylation sites in ephrinB2 are required for hippocampal long-term potentiation but not long-term depression. J Neurosci. 2007; 27:11279–11288. [PubMed: 17942722]
17. Kullander K, et al. Kinase-dependent and kinase-independent functions of EphA4 receptors in major axon tract formation in vivo. Neuron. 2001; 29:73–84. [PubMed: 11182082]
18. Tsien JZ, et al. Subregion- and cell type-restricted gene knockout in mouse brain. Cell. 1996; 87:1317–1326. [PubMed: 8980237]
19. Carmona MA, Murai KK, Wang L, Roberts AJ, Pasquale EB. Glial ephrin-A3 regulates hippocampal dendritic spine morphology and glutamate transport. Proceedings of the National Academy of Sciences of the United States of America. 2009
20. Tremblay ME, et al. Localization of EphA4 in axon terminals and dendritic spines of adult rat hippocampus. The Journal of comparative neurology. 2007; 501:691–702. [PubMed: 17299751]
21. Albensi BC, Oliver DR, Toupin J, Odero G. Electrical stimulation protocols for hippocampal synaptic plasticity and neuronal hyper-excitability: are they effective or relevant? Experimental neurology. 2007; 204:1–13. [PubMed: 17258711]
22. Beart PM, O'Shea RD. Transporters for L-glutamate: an update on their molecular pharmacology and pathological involvement. British journal of pharmacology. 2007; 150:5–17. [PubMed: 17088867]
23. Liu G, Choi S, Tsien RW. Variability of neurotransmitter concentration and nonsaturation of postsynaptic AMPA receptors at synapses in hippocampal cultures and slices. Neuron. 1999; 22:395–409. [PubMed: 10069344]
24. Oliet SH, Piet R, Poulain DA. Control of glutamate clearance and synaptic efficacy by glial coverage of neurons. Science (New York, NY. 2001; 292:923–926.

25. Tsukada S, Iino M, Takayasu Y, Shimamoto K, Ozawa S. Effects of a novel glutamate transporter blocker, (2S, 3S)-3-[3-[4-(trifluoromethyl)benzoylamino]benzyloxy]aspartate (TFB-TBOA), on activities of hippocampal neurons. Neuropharmacology. 2005; 48:479–491. [PubMed: 15755476]
26. Nolte C, et al. GFAP promoter-controlled EGFP-expressing transgenic mice: a tool to visualize astrocytes and astrogliosis in living brain tissue. Glia. 2001; 33:72–86. [PubMed: 11169793]
27. Rothstein JD, et al. Knockout of glutamate transporters reveals a major role for astroglial transport in excitotoxicity and clearance of glutamate. Neuron. 1996; 16:675–686. [PubMed: 8785064]
28. Tanaka K, et al. Epilepsy and exacerbation of brain injury in mice lacking the glutamate transporter GLT-1. Science (New York, NY. 1997; 276:1699–1702.
29. Watanabe T, et al. Amygdala-kindled and pentylenetetrazole-induced seizures in glutamate transporter GLAST-deficient mice. Brain research. 1999; 845:92–96. [PubMed: 10529447]
30. Greenwood SM, Connolly CN. Dendritic and mitochondrial changes during glutamate excitotoxicity. Neuropharmacology. 2007; 53:891–898. [PubMed: 18031769]
31. Feng G, et al. Imaging neuronal subsets in transgenic mice expressing multiple spectral variants of GFP. Neuron. 2000; 28:41–51. [PubMed: 11086982]
32. Hasbani MJ, Schlief ML, Fisher DA, Goldberg MP. Dendritic spines lost during glutamate receptor activation reemerge at original sites of synaptic contact. J Neurosci. 2001; 21:2393–2403. [PubMed: 11264313]
33. Lu YM, et al. Mice lacking metabotropic glutamate receptor 5 show impaired learning and reduced CA1 long-term potentiation (LTP) but normal CA3 LTP. J Neurosci. 1997; 17:5196–5205. [PubMed: 9185557]
34. Mulholland PJ, et al. Glutamate transporters regulate extrasynaptic NMDA receptor modulation of Kv2.1 potassium channels. J Neurosci. 2008; 28:8801–8809. [PubMed: 18753382]
35. Wadiche JI, Jahr CE. Patterned expression of Purkinje cell glutamate transporters controls synaptic plasticity. Nature neuroscience. 2005; 8:1329–1334.
36. Nikkuni O, Takayasu Y, Iino M, Tanaka K, Ozawa S. Facilitated activation of metabotropic glutamate receptors in cerebellar Purkinje cells in glutamate transporter EAAT4-deficient mice. Neuroscience research. 2007; 59:296–303. [PubMed: 17727989]
37. Levenson J, et al. Long-term potentiation and contextual fear conditioning increase neuronal glutamate uptake. Nature neuroscience. 2002; 5:155–161.
38. Nishida H, Okabe S. Direct astrocytic contacts regulate local maturation of dendritic spines. J Neurosci. 2007; 27:331–340. [PubMed: 17215394]
39. Nestor MW, Mok LP, Tulapurkar ME, Thompson SM. Plasticity of neuron-glial interactions mediated by astrocytic EphARs. J Neurosci. 2007; 27:12817–12828. [PubMed: 18032653]
40. Diamond JS, Jahr CE. Synaptically released glutamate does not overwhelm transporters on hippocampal astrocytes during high-frequency stimulation. Journal of neurophysiology. 2000; 83:2835–2843. [PubMed: 10805681]
41. Lehre KP, Rusakov DA. Asymmetry of glia near central synapses favors presynaptically directed glutamate escape. Biophysical journal. 2002; 83:125–134. [PubMed: 12080105]
42. Morris RG, et al. Elements of a neurobiological theory of the hippocampus: the role of activity-dependent synaptic plasticity in memory. Philosophical transactions of the Royal Society of London. 2003; 358:773–786. [PubMed: 12744273]
43. Tsuda H, et al. The amyotrophic lateral sclerosis 8 protein VAPB is cleaved, secreted, and acts as a ligand for Eph receptors. Cell. 2008; 133:963–977. [PubMed: 18555774]

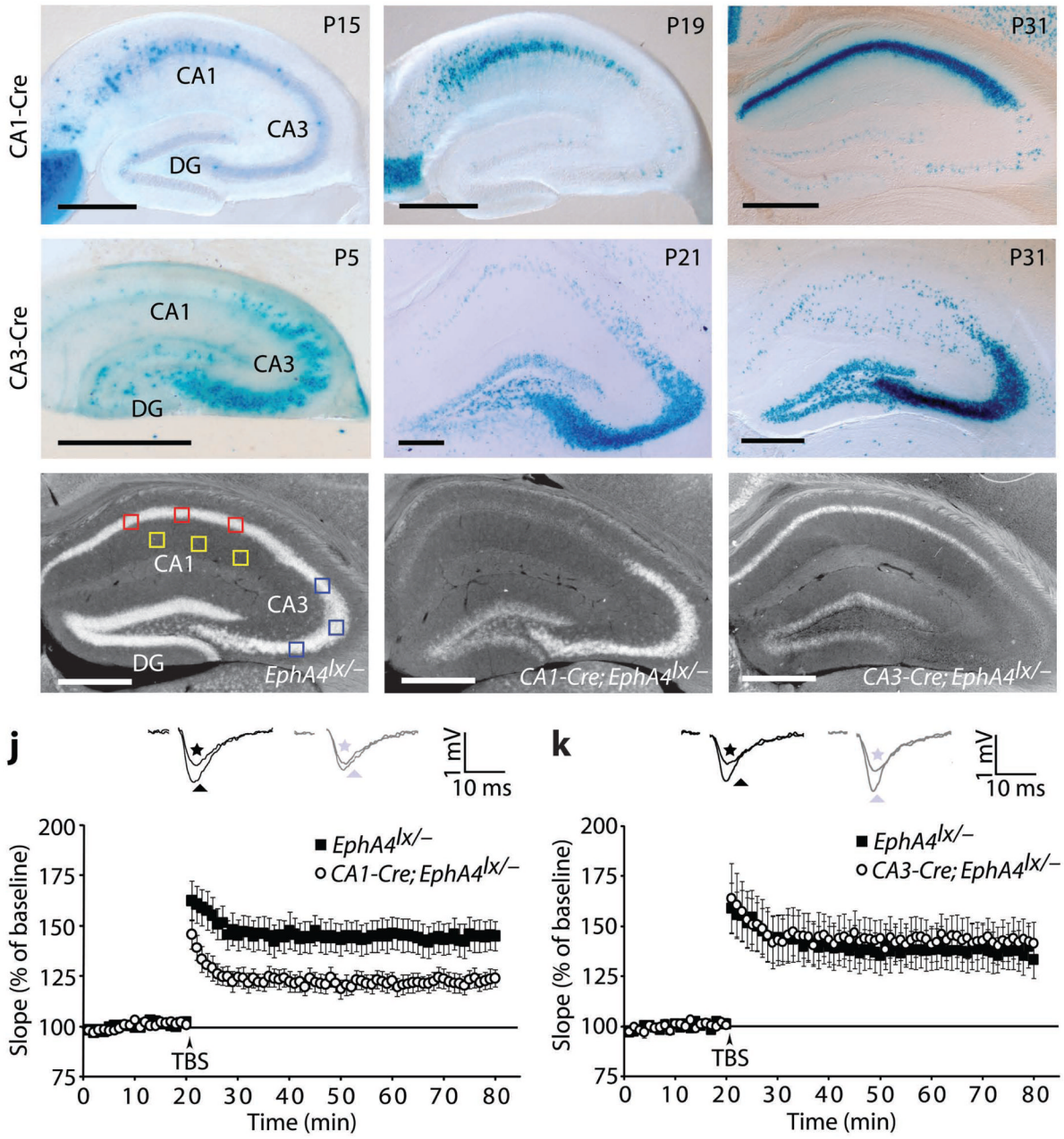

Fig. 1.

EphA4 is required for LTP in post-synaptic CA1 cells. **a–f,** Xgal staining of hippocampal sections of the indicated postnatal (P) ages (days) of *CA1-Cre;Rosa26*$^{lx/+}$ (**a–c**) and *CA3-Cre;Rosa26*$^{lx/+}$ (**d–f**) mice. CA1, *cornu ammonis* 1; CA3, *cornu ammonis* 3; DG, dentate gyrus. **g–i,** *In situ* hybridizations for EphA4 mRNA in adult hippocampus from mice of the indicated genotypes. The small squares indicate the regions used for densitometric measurements for the calculation of the recombination efficiency. Red squares, CA1; blue squares, CA3; yellow squares, background. Scale bars: 500 μm. Recombination efficiencies of CA1-Cre and CA3-Cre in CA1 and CA3, respectively was approximately 80% (see text) and of CA3-Cre in dentate gyrus was 36% (data not shown). **j,k,** Scatter plots showing LTP, represented as a percentage of the baseline, induced by stimulation of presynaptic CA3

neurons with three TBS. Insets: representative traces from controls (black) and mutants (gray) recorded before (stars) and 55–60 min after (triangles) LTP induction. For reasons of clarity the stimulation artifact was removed. **j,** *CA1-Cre;EphA4*$^{lx/-}$ mice show a marked deficit in early CA3-CA1 LTP compared to littermate *EphA4*$^{lx/-}$ controls (123.0 ± 4.4% in mutants, n=12 slices, 7 mice versus 144.8 ± 7.6% in controls, n=14 slices, 7 mice, at 55–60 min after stimulus, *t*-test, p=0.02). **k,** *CA3-Cre;EphA4*$^{lx/-}$ mice show normal TBS-induced LTP (142.9 ± 10.0% in mutants, n=10 slices, 8 mice, versus 136.9 ± 9.7% in controls, n=10 slices, 8 mice, at 55–60 min after stimulus, *t*-test, p=0.7). Error bars: s.e.m.

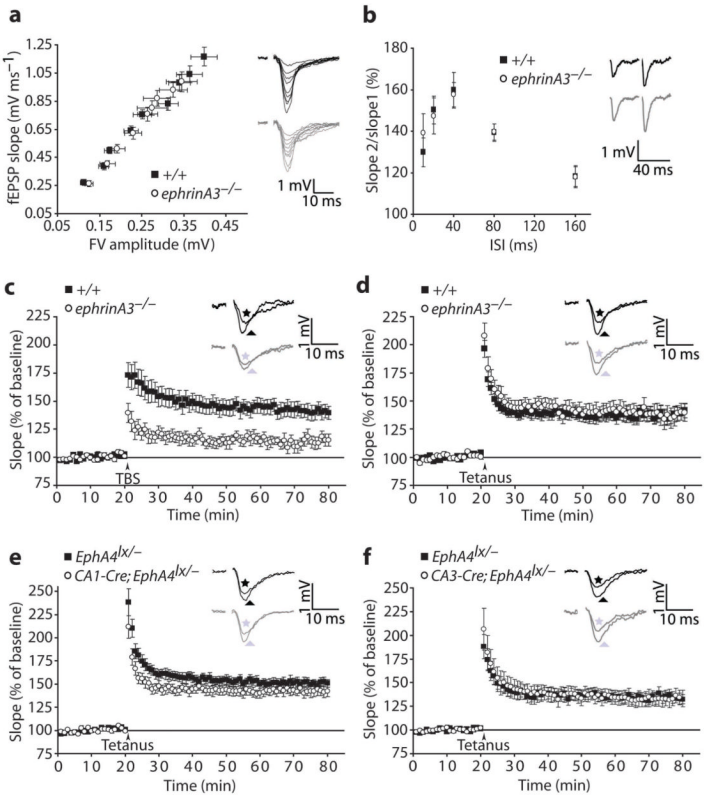

Fig. 2.

EphrinA3 is required for TBS-induced LTP. **a,** fEPSPs slopes at various stimulus intensities (FV, fiber volley) and representative traces (+/+, black; ephrinA3, gray, n=12 slices, 6 mice per group, ANCOVA, p=0.1). **b,** PPF at various ISIs and representative traces at 40 ms ISI (+/+, black; ephrinA3, gray, n=10 slices, 5 mice per group, two-way repeated measures ANOVA, between genotypes: F(1, 90)=0.03, p=0.9). **c–f,** Scatter plots showing LTP induced by stimulation of presynaptic CA3 neurons with three TBS (**c**) or a single tetanus (**d–f**). **c,** *ephrinA3*$^{-/-}$ mice show a strong deficit in TBS-induced LTP compared to +/+ controls (+/+, 140.7 ± 6.1%, n=14 slices, 10 mice; *ephrinA3*$^{-/-}$, 114.8 ± 5.0% n=12 slices, 10 mice, at 55–60 min after stimulus, *t*-test, p=0.004). **d,** *ephrinA3*$^{-/-}$ mice show normal tetanus-induced LTP (+/+, 138.6 ± 6.0%, n=13 slices, 10 mice; *ephrinA3*$^{-/-}$, 137.9 ± 7.7% n=12 slices, 10 mice, at 55–60 min after stimulus, *t*-test, p=0.9). **e,** *CA1-Cre;EphA4*$^{lx/-}$ mice show normal tetanus-induced LTP (142.8 ± 6.0% in mutants, n=11 slices, 9 mice, versus 151.0 ± 11.0% in controls, n=12 slices, 9 mice, at 55–60 min after stimulus, *t*-test, p=0.5). **f,** *CA3-Cre;EphA4*$^{lx/-}$ mice have normal tetanus-induced LTP (133.8 ± 7.9% in mutants, n=10 slices, 8 mice, versus 134.0 ± 5.4% in controls, n=9 slices, 8 mice, at 55–60 min after stimulus, *t*-test, p=1.0). Insets: representative traces from controls (black) and mutants (gray) recorded before (stars) and 55–60 min after (triangles) LTP induction. The stimulation artifacts were removed. Error bars: s.e.m.

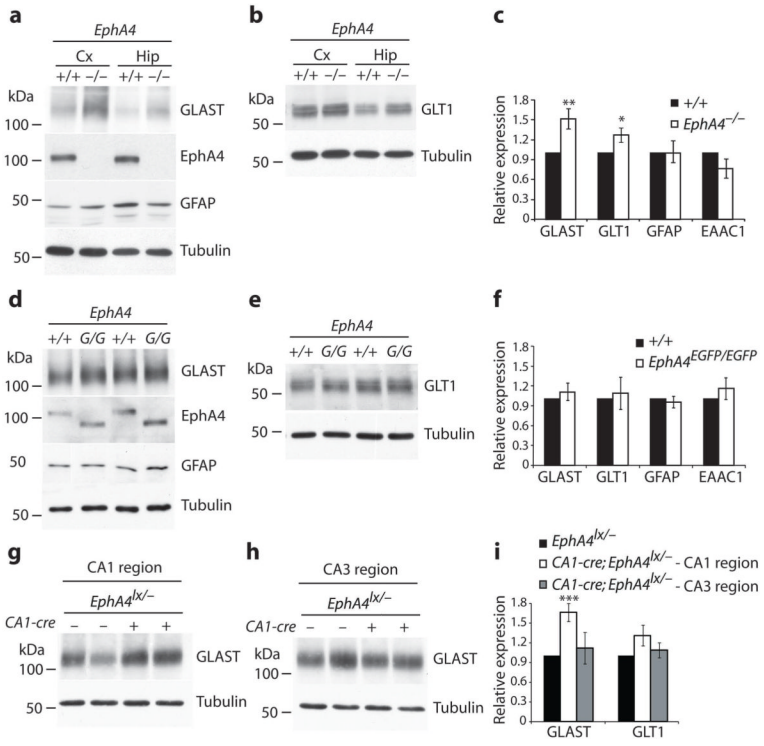

Fig. 3.

Upregulation of GLAST and GLT-1 protein levels in *EphA4* mutants. **a,b,** Protein lysates from cerebral cortex (Cx) and hippocampus (Hip) derived from *EphA4*$^{-/-}$ and littermate +/+ controls were compared by western blot analysis for their content of GLAST, GLT-1, GFAP, EAAC1, EphA4 and Tubulin. **c,** Quantification of glutamate transporter levels and GFAP in hippocampi of *EphA4*$^{-/-}$ and littermate +/+ controls. Expression levels were normalized to Tubulin levels by densitometric measurements. Mean values of intensities of the indicated proteins are shown relative to levels in +/+ protein lysates. GLAST and GLT1 levels were increased by 50% and 25% respectively in *EphA4*$^{-/-}$ mice (GLAST **p=0.009, n=10 mice per group; GLT1 *p=0.03, n=15 mice, GFAP p=0.2, n=10 mice; EAAC1 p=0.3, n=3 mice, *t*-test) compared to +/+ controls. **d,e,** Western blot analysis of hippocampal protein lysates from *EphA4*$^{EGFP/EGFP}$ (G/G) and littermate +/+ controls for their content of GLAST, GLT-1, GFAP, EphA4 and Tubulin. **f,** Quantification of protein levels calculated as in (**c**) (n=7–9 mice per group, p>0.3, *t*-test). **g,h,** Western blot analysis of protein lysates from dissected CA1 and CA3 regions derived from *CA1-Cre;EphA4*$^{lx/-}$ mice or *EphA4*$^{lx/-}$ controls for their content of GLAST and Tubulin. **i,** GLAST levels in CA1, but not CA3 were increased to the same extend as in *EphA4*$^{-/-}$ (GLAST in CA1, n=7 mice, ***p=0.0009; GLAST in CA3, n=6 mice, p=0.7; GLT1 in CA1, n=13 mice, p=0.07; GLT1 in CA, n=6 mice, p=0.5; and GFAP, n=6 mice, p=0.9, *t*-test). Error bars: s.e.m.

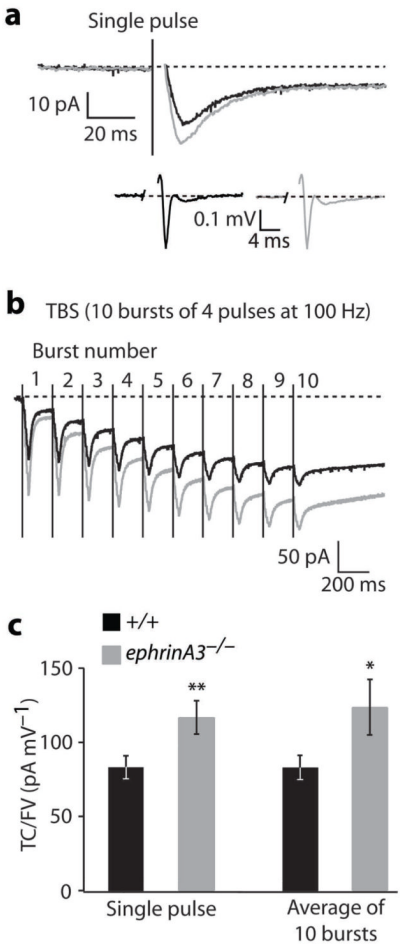

Fig. 4.

Astrocytic glutamate transporter currents. **a,** Mean inward currents in response to a single pulse stimulation of Schaffer collaterals in +/+ (black) and *ephrinA3*$^{-/-}$ mice (gray). The slow, persistent component did not differ between +/+ and *ephrinA3*$^{-/-}$ animals. Inset shows mean fiber volleys in +/+ (black) and ephrinA3$^{-/-}$ (gray) animals (the peaks of individual traces were aligned in time, before calculating the average). **b,** Mean inward currents in response to TBS in +/+ animals (black) and *ephrinA3*$^{-/-}$ animals (gray). Traces are averages from all performed stimulations. The stimulation artifacts in **a** and **b** were replaced by a vertical line indicating the start of the stimulation. **c,** Bar chart illustrating mean glutamate transporter currents amplitudes (TC), normalized to the amplitude of the corresponding fiber volleys (FV). Each transporter current amplitude was divided by the amplitude of the corresponding FV in order to normalize for the numbers of fibers activated. Transporter currents in *ephrinA3*$^{-/-}$ animals were significantly higher than in +/+ controls in response to a single pulse stimulation (117.7 ± 11.1 pA mV^{-1} in mutants, n=42 recordings, 20 cells, versus 95.7 ± 8.9 pA mV^{-1} in +/+ controls, 34 recordings, 17 cells, **p=0.01, *t*-test) and in response to TBS (124.8 ± 18.8 pA mV^{-1} in mutants, n=20 measurements, 15 cells, and 83.5 ± 8.5 pA mV^{-1} in +/+ controls, n=18 measurements, 10 cells; *p=0.03, *t*-test). Error bars: s.e.m.

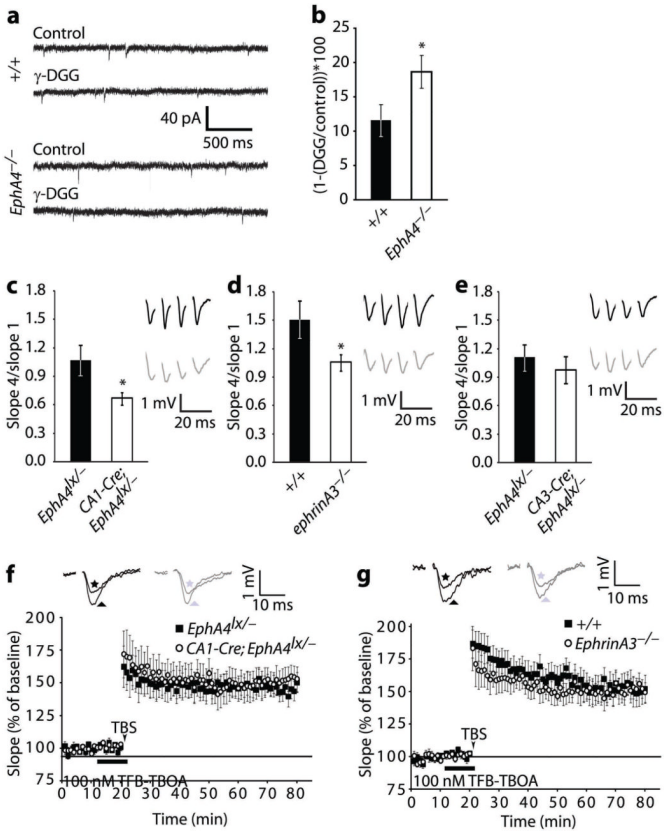

Fig. 5.

Glutamate levels, post-synaptic responses to high frequency stimulation and pharmacological rescue of LTP. **a,** Representative traces of mEPSCs in +/+ and *EphA4*$^{-/-}$ mice in absence and presence of 1 mM γ-DGG. **b,** Histogram illustrating the inhibitory effect of γ-DGG on mean mEPSCs amplitude in *EphA4*$^{-/-}$ mice and controls. Inhibition was stronger in *EphA4*$^{-/-}$ slices than in +/+ controls (18.6%±2.4% versus 11.6%±2.3%, *p=0.04, *t*-test; n=13 mice per group). **c–e**, Histograms depicting the fEPSP slope4/slope1 ratio during a train of four stimuli at 100Hz (0.67±0.07 in *CA1-Cre;EphA4*$^{lx/-}$, n=12 slices, 7 mice. 1.07±0.16 in *EphA4*$^{lx/-}$, n=14 slices, 7 mice, p=0.03; 1.06±0.09 in *ephrinA3*$^{-/-}$, n=14 slices, 9 mice, 1.51±0.2 in +/+, n=13 slices, 9 mice, p=0.05; 0.98±0.14 in *CA3-Cre;EphA4*$^{lx/-}$, n=9 slices, 6 mice, 1.12±0.13 in *EphA4*$^{lx/-}$, n=10 slices, 6 mice, p=0.5, *t*-test). Insets: traces from one representative train in controls (black) and mutants (gray). The stimulation artifacts were removed. **f,g,** Graphs showing TBS-induced LTP in presence of TFB-TBOA (applied 8 min before TBS and washed-out 2 min after) in *CA1-Cre;EphA4*$^{lx/-}$ (**f**) and *ephrinA3*$^{-/-}$ (**g**) mice. (153.5±9.1% in *CA1-Cre;EphA4*$^{lx/-}$, n=9 slices, 7 mice, 145.2±6.7% in *EphA4*$^{lx/-}$, n=10 slices, 7 mice, p=0.6; 152.6 ± 7.6% in *ephrinA3*$^{-/-}$, n=11 slices, 9 mice, 149.9±10.1% in +/+, n=10 slices, 9 mice, p=0.8, *t*-test). Insets: representative traces from controls (black) and mutants (gray) recorded before (stars) and 55–60 min after (triangles) LTP induction. The stimulation artifacts were removed. Error bars: s.e.m.

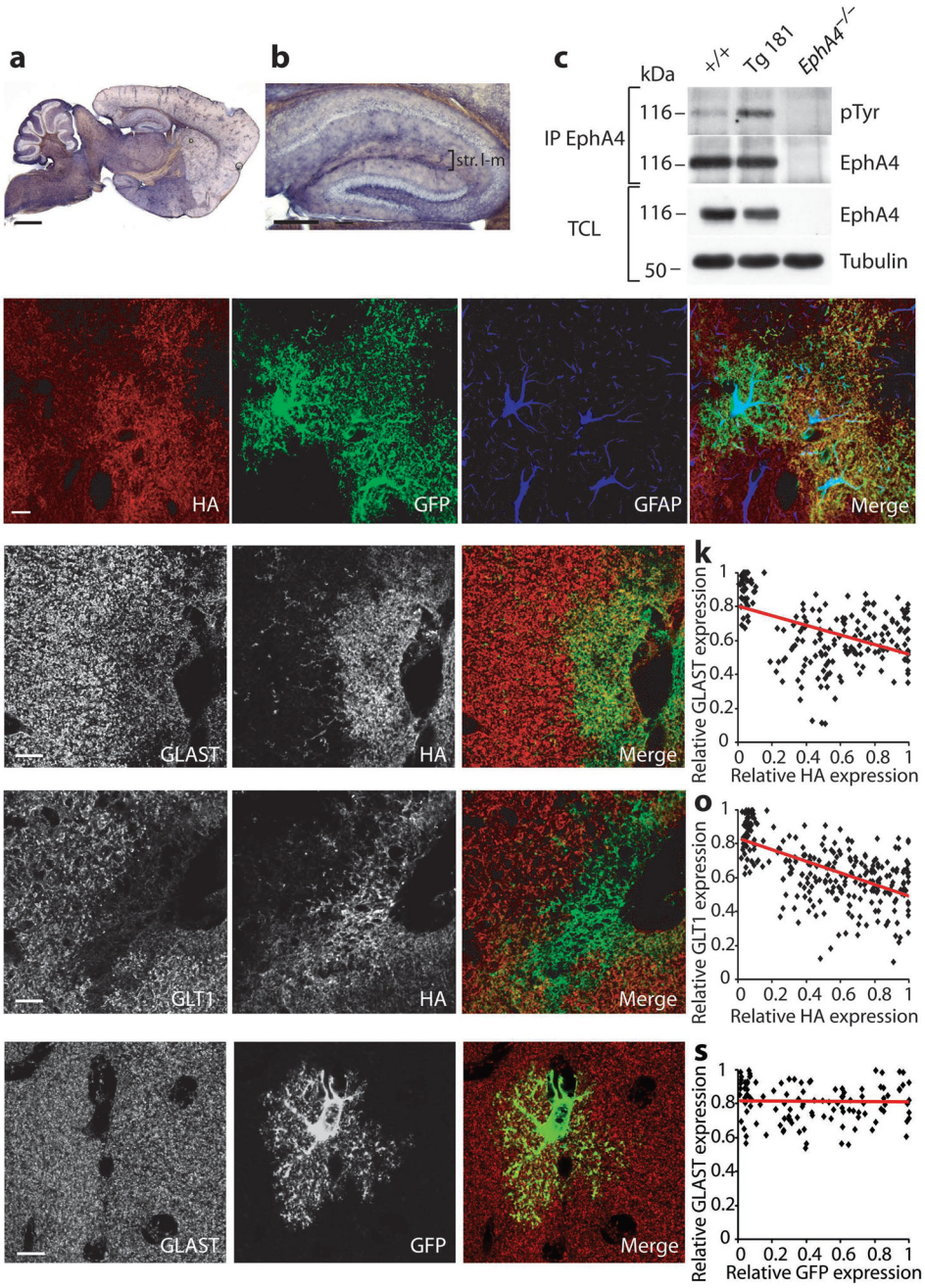

Fig. 6.

EphrinA3 overexpression in astrocytes reduces glutamate transporters. **a,b** Anti-HA immunohistochemistry from Tg181 showing scattered distribution of transgenic protein throughout the brain and hippocampus. **c,** Transgenic ephrinA3 induces higher endogenous phosphorylation of EphA4. EphA4 was immunoprecipitated (IP) from +/+ and Tg181 hippocampal lysates, and blotted with pTyr and EphA4 antibodies. *EphA4*$^{-/-}$ hippocampal lysates were used as control. Total cell lysates (TCL) of the same fractions show EphA4 and Tubulin levels. **d–g,** Specific expression of transgenic ephrinA3 in glial cells. Immunofluorescence confocal images of hippocampal sections from adult Tg181 crossed to a GFAP-GFP line [26]. Triple labeling for the indicated proteins show colocalization of HA

with GFP but not with the cytoplasmic marker GFAP (**g**) indicating that the transgenic protein is expressed in fine processes of astrocytes. **h–j, l–n,** Immunofluorescence single plane confocal images showing double labeling for GLAST/HA (**h–j**) and GLT1/HA (**l–n**) in the *stratum lacunosum-moleculare* from Tg181. **k,o,** Scatter plots showing the negative correlation between GLAST/HA (**k**) and GLT1/HA relative pixel intensities (**o**) (GLAST/HA correlation factor=−0.46, n=198 regions, 3 mice; GLT1/HA correlation factor=−0.58, n=280 regions, 3 mice, *t*-test, $p<0.0001$). Linear regression lines are represented in red. **p–r,** Immunofluorescence single plane confocal images showing double-labeling for GLAST/GFP in GFAP-GFP mice. Expression of GLAST (red) is not affected in locations where the levels of transgenic GFP (green) are high. **s,** Scatter plot showing no correlation between GLAST/GFP relative pixel intensities (correlation factor=−0.02, n=121 regions, 2 mice, *t*-test, $p>0.1$). Scale bars: c, 1 mm; d, 300 μm; e–n, 10 μm.

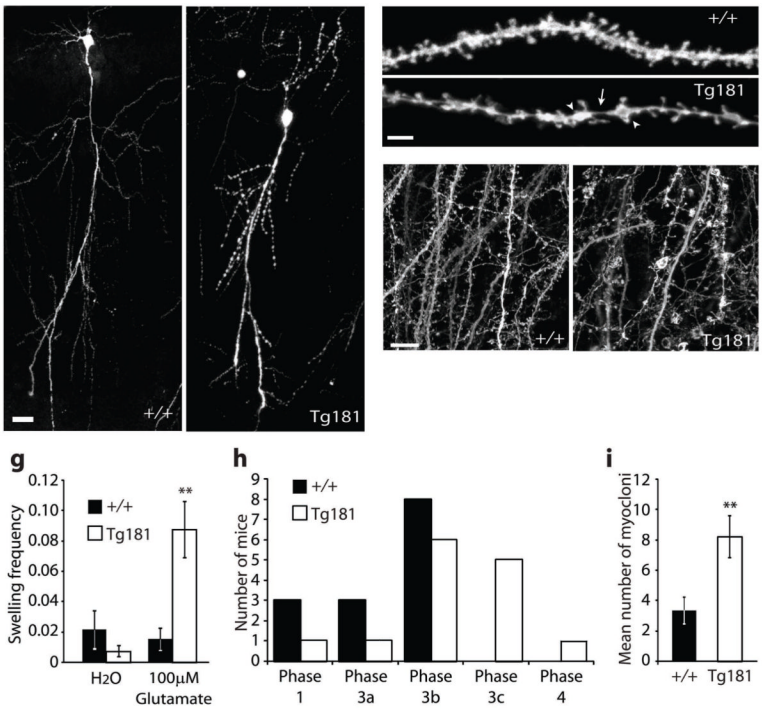

Fig. 7.

EphrinA3 overexpression in astrocytes increases susceptibility to excitotoxicity and seizures. **a,b,** Transgenic ephrinA3 causes dendritic beading. Confocal images of single CA1 pyramidal neurons from +/+ (**a)** and Tg181 (**b**) mice crossed to GFP-M mice [31]. **c,d,** Confocal stack of stretches of dendrite of CA1 neurons from +/+ (**c**) and Tg181(**d**) mice labeled with DiI; arrowheads point to focal swellings, arrow points to the thin dendritic stretch separating the swellings. **e,f,** Confocal stacks of CA1 pyramidal dendrites in organotypic slices from +/+ (**e)** and Tg181 (**f**) mice crossed to GFP-M mice treated with 100 μM glutamate. **g,** Bar graph showing the swelling frequency (expressed as number of swellings/dendrite complexity index) in control (H_2O) and treated slices. In Tg181 mice there is 5.7-fold increase in swelling frequency compared to +/+ controls (0.088 ± 0.018, n=6 slices, 3 mice, in Tg181 versus 0.015 ± 0.007, n=7 slices, 3 mice, in littermate control +/+ animals, *t*-test, **p=0.002). **h,** PTZ-induced epileptic seizures, depicted as maximal phase reached after intra peritoneal injection of 45 mg/kg PTZ, were more severe in Tg 181 mice than in +/+ mice (n=14 mice, p=0.01, Mann–Whitney *U*-test). Phase classification was performed as described [44]. **i,** Mean number of whole-body myocloni in phase 3 after injection of 45 mg/kg PTZ (3.42 ± 0.82 in +/+ mice, n=12 mice versus 8.25 ± 1.39 in Tg181 mice, n=12, *t*-test, **p=0.009). Scale bars: **a,b,** 50 μm; **c,d,** 5 μm; g, h, 10 μm. Error bars: s.e.m.